Breast Imaging with Fluorine-18-FDG PET: Quantitative Image Analysis

Norbert Avril, Sandra Bense, Sibylle I. Ziegler, Jörg Dose, Wolfgang Weber, Christian Laubenbacher, Wolfgang Römer, Fritz Jänicke and Markus Schwaiger

Departments of Nuclear Medicine and Gynecology, Technical University of Munich, Munich, Germany

This study evaluated various quantitative criteria for analysis of breast imaging with PET using the radiolabeled glucose analog ^{18}F-fluorodeoxyglucose (FDG). **Methods:** In a prospective study, 73 patients with abnormal mammography or palpable breast masses scheduled for biopsy were investigated with PET. A total of 97 breast tumors were evaluated by histology, including 46 benign and 51 malignant tumors. Using a whole-body PET scanner, attenuation-corrected images were acquired between 40 and 60 min after tracer injection. For Patlak analysis, dynamic data acquisition was obtained in 24 patients. To differentiate between benign and malignant breast tumors, receiver operating characteristic curves were calculated using incrementally increasing threshold values for tumor/nontumor ratios based on average and maximum activity values per region of interest, standardized uptake values (corrected for partial volume effect, normalized to blood glucose, partial volume effect and blood glucose, using the lean body mass as well as the body surface area) and calculating the FDG influx rate (K) assessed by Patlak analysis. **Results:** Quantification of FDG uptake in breast tumors provided objective criteria for differentiation between benign and malignant tissue with similar diagnostic accuracy as compared with visual analysis. Applying correction for partial volume effect and normalization by blood glucose yielded the highest diagnostic accuracy. **Conclusions:** These quantitative methods provided accurate evaluation of PET data for differentiating benign from malignant breast tumors. Quantitative assessment is recommended to complement visual image interpretation with the potential benefit of reduced interobserver variability.

Key Words: PET; fluorine-18-FDG; breast cancer; quantitative image analysis

J Nucl Med 1997; 38:1186–1191

Metabolic imaging with PET and the radiolabeled glucose analog ^{18}F-fluorodeoxyglucose (FDG) has been introduced as a promising technique for identification of breast cancer (*1–8*). Differentiation between benign and malignant breast abnormalities by means of noninvasive diagnostic procedures still remains an unsolved problem. Using mammography, sensitive detection of breast cancer can be achieved only at a high rate of false-positive results (*9*). In a previous study including 51 patients, we evaluated the role of PET imaging for differentiating between benign and malignant breast abnormalities (*8*). By visual image interpretation, FDG uptake in breast tissue was classified into three categories (negative, probable and definite positive). Considering only "definite" FDG uptake to represent malignancy, a sensitivity of 68% and a specificity of 97% was recorded. Sensitivity increased to 83% and specificity declined to 84% if "probable" findings were regarded as positive.

Scintigraphic information may be analyzed either by visual interpretation or by additionally obtaining regional tracer uptake. Depending on the individual experience of the observer, visual analysis leads to identification of abnormalities in regional tracer distribution. In contrast, quantitative parameters offer more objective and observer-independent criteria. Several methods have been suggested for analysis of PET studies in oncology (*10–18*). Dose uptake ratios, standardized uptake value (SUV), standardized uptake ratio, differential uptake ratio and differential absorption ratio have been introduced to normalize tracer uptake to injected dose and body weight (*16,17,19–24*). However, there are no generally accepted methods established for quantitative analysis of PET imaging. The aim of this study was to evaluate the diagnostic accuracy of various quantitative analysis approaches. Using the region of interest (ROI) technique, ROIs were placed over histologically proven breast masses to determine regional FDG uptake. Receiver operating characteristic (ROC) curves were calculated using incrementally increasing cutoff values to differentiate between benign and malignant breast tumors.

MATERIALS AND METHODS

Patients

Seventy-three patients with abnormal mammography or palpable breast masses, who were scheduled to undergo breast surgery, were referred for PET imaging. In these patients, a total of 97 breast tumors were evaluated by histology. Details of the study were explained by a physician and written informed consent was obtained from all patients. The study was approved by the committee for human research at our hospital. Patients were not included in the study if they were pregnant, had known diabetes or were younger than 18 yr. Patients with prior therapy within 3 mo, e.g., chemotherapy and surgery or radiation therapy of the breast, were also excluded. Mean age was 50 ± 11.4 yr (mean ± s.d.), ranging from 18 to 74 yr. Thirty-two patients were premenopausal, 10 perimenopausal and 31 postmenopausal. Patients fasted for at least 4 hr before PET imaging. The serum glucose level was measured with blood glucose reagent strips and photometric measurement. Mean blood glucose level was 75 mg/100 ml (range 44–126).

PET Imaging

PET scans were performed using a whole-body PET scanner. Emission data corrected for randoms, dead time and attenuation were reconstructed with filtered back-projection (Hanning filter with a cutoff frequency of 0.4 cycle per pixel). In all patients, transmission scans with Germanium-68 rod sources were performed for 15 min, yielding approximately 4 million counts per slice. FDG was produced by nucleophilic fluorination with a method modified from the synthesis of Hamacher (*25*). Isotopic purity, radiochemical purity, sterility and pyrogenicity were tested for all FDG doses.

All patients were studied in the prone position with both arms at their sides. For positioning, a foam cushion on the scanner table was used with a hole that allows the breasts to be unconstrained. In 24 patients, dynamic data acquisition (12 frames) was obtained for up to 60 min after intravenous administration of 270–390 MBq

Received July 26, 1996; revision accepted Jan. 13, 1997.

For correspondence or reprints contact: Dr. Norbert Avril, Nuklearmedizinische Klinik und Poliklinik, Technical University of Munich, Klinikum rechts der Isar, Ismaningstrasse 22, 81675, Munich, Germany.

TABLE 1
Statistical Data for Quantitative Analysis of FDG Uptake in Breast Tumors

	T/NT [av]	T/NT [max]	SUV [av]	SUV [av-pv]	SUV [av-glc]	SUV [av-pv-glc]	SUV [max]	SUV [max-pv]	SUV [max-glc]	SUV [max-pv-glc]	SUV [av-lean]	SUV [av-bsa]	Patlak (K) ml/min/100 g
	(n = 40)		Benign breast tumors (n = 46)										(n = 12)
Mean ± s.d.	1.3 ± 0.4	1.5 ± 0.6	1.4 ± 0.5	1.5 ± 0.7	1.0 ± 0.4	1.1 ± 0.6	1.9 ± 0.6	2.0 ± 0.9	1.4 ± 0.5	1.5 ± 0.7	1.3 ± 0.5	3.8 ± 1.4	1.0 ± 1.0
s.d. (%)	31%	40%	36%	50%	40%	58%	32%	43%	36%	51%	37%	35%	100%
Range	0.5–3.0	0.7–2.2	0.3–2.3	0.3–5.2	0.2–2.3	0.2–4.4	0.9–3.1	0.9–6.3	0.6–2.5	0.6–5.4	0.2–2.3	0.7–6.8	0.3–2.0
	(n = 43)		Breast cancer (n = 51)										(n = 23)
Mean ± s.d.	3.0 ± 2.3	4.0 ± 3.5	3.6 ± 2.5	4.2 ± 2.6	2.7 ± 1.9	3.2 ± 2.0	4.3 ± 3.0	5.1 ± 3.1	3.3 ± 2.3	3.9 ± 2.4	3.0 ± 2.0	9.2 ± 6.0	2.0 ± 1.0
s.d. (%)	77%	88%	71%	60%	70%	62%	70%	61%	70%	62%	65%	66%	50%
Range	1.0–11.2	1.2–17.9	0.4–11.7	0.4–12.7	0.3–9.3	0.3–10.2	0.7–14.1	0.7–15.4	0.6–11.2	0.5–12.4	0.4–9.6	1.1–29.6	0.4–7.0

Malignant tumors had significantly higher values compared to benign lesions ($p < 0.01$) for all methods tested.

(approximately 10 mCi) [^{18}F]FDG. In 49 patients, static emission scans from 40 to 60 min after tracer injection were obtained. Transmission scans were acquired before or after tracer injection in dynamic or static imaging protocols, respectively.

Data Analysis

ROIs were manually placed over all histologically proven breast lesions to determine regional FDG uptake. For lesions appearing with focally increased FDG uptake, a ROI was drawn exactly around the tumor. For lesions that could not be clearly identified by increased FDG uptake, mammography as well as the surgeon's report were additionally used for the positioning of the ROI.

Tumor/nontumor ratios were calculated between lesions and contralateral breast tissue for average (T/NT [av]) and maximum activity values (T/NT [max]) of each ROI. Ratios were not obtained in patients with prior breast surgery or additional breast abnormalities at the contralateral breast. SUVs were calculated by normalization to injected dose and body weight using average (SUV [av]) and maximum activity (SUV [max]) values of each ROI. Partial volume correction was used for lesions with focally increased FDG uptake. The tumor size was obtained by analysis of the axial activity profile of the lesions (*26*). An optimal threshold for estimating the tumor diameter was found at 70% of the maximum activity values within a lesion showing a high correlation compared with the tumor size obtained by histology ($r = 0.91$) (*27*). Correction factors for partial volume effect have been measured with phantoms simulating tumor uptake by radioactive spheres of known dimensions and various background activities (ranging from 5% to 50%). Based on these data, appropriate recovery coefficients were used to correct SUVs for partial volume effect (SUV [av-pv] and SUV [max-pv]). Furthermore, SUV values were normalized to blood glucose (SUV [av-glc], SUV [max-glc]), as well as to both partial volume effect and blood glucose (SUV [av-pv-glc], SUV [max-pv-glc]). Normalization to blood glucose was performed by multiplying SUVs with the blood glucose level and using 100 mg/100 ml as reference (SUV [glc]). Lean SUV values were calculated by normalizing ROI activity values to injected dose and lean body mass (SUV [av-lean]). The lean body mass was estimated using the formula [45.5 + 0.91 * [patient height (cm) − 152]] (*14*). For SUVs [av-bsa], the body surface area instead of the patients weight was used [(m^2) = (weight in kg)$^{0.425}$ * (height in cm)$^{0.725}$ * 0.007184] (*15*). Dynamic PET studies allow for the assessment of the FDG influx constant using the Patlak analysis approach (*10*). The arterial input function was obtained with a ROI placed in the left ventricular cavity. The slope of the linear part of the curve determined the FDG influx constant (K), expressed as milliliters per min/100 g tissue. Dynamic data acquisition was available for 35 histologically proven breast tumors (24 patients).

Statistical Analysis

The ability of FDG-PET to differentiate between benign and malignant breast tumors was determined by calculating the areas under ROC curves (*28*). ROC curve analysis was performed using the Clabroc-program of Charles E. Metz (Apple Macintosh™ version, January 1991, Department of Radiology, University of Chicago) by incrementally increasing the threshold for separating benign from malignant lesions and recalculating sensitivity and specificity after each increment. A modified Student's t-test was used to determine if there were statistically significant differences between the area under the ROC curves (*29*). For statistical evaluation of SUVs in benign and malignant lesions, the Mann-Whitney U test was used.

RESULTS

Forty-six benign breast masses and 51 malignant breast tumors were found in histology. Mean size was 2.5 ± 0.9 cm for benign (range 1.0–5.0 cm) and 2.7 ± 1.7 cm for malignant tumors (range 0.6–9 cm). Benign breast masses consisted mainly of fibrocystic or proliferative breast disease (n = 34) and fibroadenomas (n = 8), as well as one case with inflammatory breast disease, focal necrosis, a ductal adenoma and a granular cell tumor. Malignant breast tumors included 33 invasive ductal carcinomas, 11 invasive lobular carcinomas, 2 medullary carcinomas, 1 mucinous carcinoma, as well as 3 ductal in situ carcinomas and 1 lobular in situ carcinoma.

Table 1 shows statistical data (mean ± s.d. and range) for various parameters used to analyze the FDG uptake in benign and malignant breast tumors. Tumor/nontumor ratios were evaluated in 62 patients with a total of 83 histologically proven breast tumors. SUVs were calculated for all patients studied (97 breast tumors in 73 patients). All parameters tested showed statistically significant higher FDG uptake in malignant compared with benign tumors ($p < 0.01$).

Reproducibility of placing ROIs over tumors was tested in a subset of 20 patients. Obtaining average activity values within a ROI, intraobserver variability ($r = 0.96$) and interobserver variability assessed by two observers ($r = 0.91$) showed high reproducibility.

Results of ROC curve analysis for various quantitative analysis methods to differentiate between benign and malignant breast tumors are shown in Figure 1 and Table 2. For SUVs, the area under the ROC curve was larger using average activity values within a ROI (SUV [av]) compared with maximum

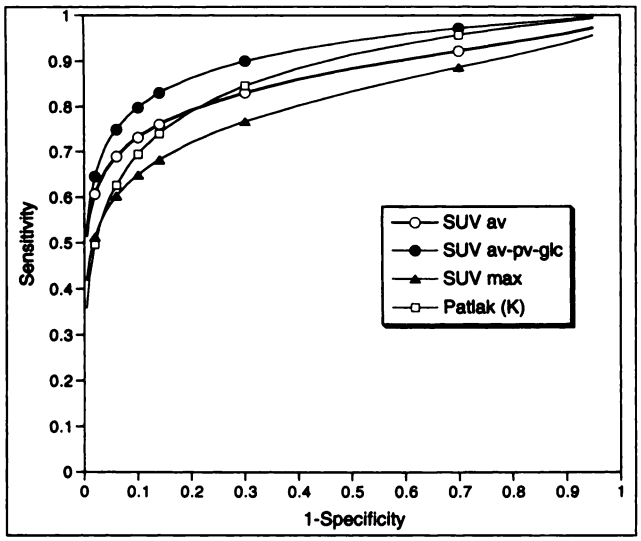

FIGURE 1. ROC curves for various quantitative analysis methods used to differentiate between benign and malignant breast tumors.

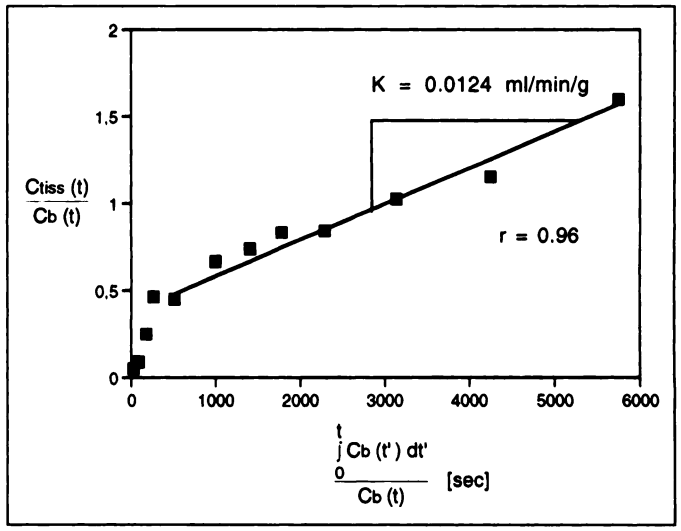

FIGURE 2. Example of a Patlak analysis plot of an invasive ductal breast carcinoma. Arterial input function was derived from the left ventricular cavity. Solid line shows linear regression (r = 0.96). Ctiss (t), tissue tracer concentration (Bq/g) at time t. Cb (t), blood tracer concentration (Bq/g) at time t. K, FDG influx rate (ml/min/g).

activity values (SUV [max]). The difference between these areas (0.86 ± 0.04 versus 0.81 ± 0.04) was statistically significant ($p = 0.03$). Using average activity values and combining correction for partial volume effect and normalization to blood glucose (SUV [av-pv-glc]) yielded the largest area under the ROC curve (0.92 ± 0.03). On the other hand, uncorrected maximum SUV values (SUV [max]) resulted in the lowest area under the ROC curve (0.81 ± 0.04). Using lean body mass, body surface area, tumor to nontumor ratios, as well as calculating the influx constant for FDG (K) provided no diagnostic advantage. Figure 2 shows an example of a Patlak analysis plot.

When analyzing the ability to characterize breast tumors as malignant at a certain specificity, the corresponding sensitivity was found to be different. Therefore, SUV cutoff values for differentiation between benign and malignant breast tumors, as well as corresponding sensitivity values at specificities of 80% and 90%, are shown in Table 3.

TABLE 2
ROC Curve Analysis for Various Quantitative Analysis Approaches and Areas Under the ROC Curve

	ROC Area ± s.d.	Compared with SUV [av]	Compared with SUV [max]
T/NT [av]	0.88 ± 0.04	ns	nd
T/NT [max]	0.86 ± 0.04	ns	nd
SUV [av]	0.86 ± 0.04	—	$p < 0.03$
SUV [av-pv]	0.91 ± 0.03	ns	nd
SUV [av-glc]	0.87 ± 0.04	ns	nd
SUV [av-pv-glc]	0.92 ± 0.03	ns	nd
SUV [av-lean]	0.85 ± 0.04	ns	nd
SUV [av-bsa]	0.87 ± 0.04	ns	nd
SUV [max]	0.81 ± 0.04	$p < 0.03$	—
SUV [max-pv]	0.87 ± 0.04	nd	$p < 0.01$
SUV [max-glc]	0.85 ± 0.04	nd	ns
SUV [max-pv-glc]	0.87 ± 0.04	nd	$p < 0.01$
Patlak (K)	0.87 ± 0.06	ns	nd

The SUV [av] and the SUV [max] areas were used as reference to test for statistically significant differences between the areas.
ns = not significant; nd = not done.

DISCUSSION

This study compared the ability of various quantitative analysis methods to differentiate between benign and malignant breast tumors using FDG-PET. ROC curves showed that maximum activity values (SUV [max]) within a user-defined ROI resulted in significantly lower diagnostic accuracy ($p < 0.03$) than using average activity values (SUV [av]). Because of higher statistical noise of SUV [max] values in benign lesions, differentiation of malignant breast tumors was less accurate (Table 3). This result is important, because it is easier to obtain maximum activity values, since it is not necessary to draw ROIs exactly around the tumor. Comparing all correction and normalization methods tested, average SUVs, corrected for partial volume effect and normalized to blood glucose (SUV [av-pv-glc]) yielded the highest diagnostic accuracy (at a specificity of 90%, the corresponding sensitivity was 85%). However, compared with SUV [av] values, there was no statistically significant difference. Using SUVs, correction for partial volume effect resulted in the most pronounced improvement in diagnostic accuracy. On the other hand, normalization to blood glucose level, using lean body mass or body surface area yielded no diagnostic advantage. Tumor/nontumor ratios provided diagnostic accuracy similar to calculating SUVs. This may be explained by relatively low and stable background activity in normal breast tissue that was used to define the

TABLE 3
Corresponding Sensitivity Values at Specificities of 80% and 90% for Various Analysis Methods Tested

	90% Specificity SUV (sensitivity, %)	80% Specificity SUV (sensitivity, %)
SUV [av]	2.1 (69)	1.8 (75)
SUV [av-pv]	2.1 (81)	1.8 (85)
SUV [av-glc]	1.5 (74)	1.3 (78)
SUV [av-pv-glc]	1.5 (85)	1.3 (90)
SUV [av-lean]	2.0 (66)	1.7 (76)
SUV [av-bsa]	5.6 (71)	5.1 (75)
SUV [max]	2.8 (66)	2.4 (71)
SUV [max-pv]	2.9 (77)	2.4 (86)
SUV [max-glc]	2.0 (72)	1.7 (78)
SUV [max-pv-glc]	2.0 (82)	1.7 (87)

"nontumor" ROI. Nevertheless, this method is limited, since all patients with additional abnormalities at the contralateral breast were not included in the tumor/nontumor ratio analysis.

Tracer Kinetics

Quantitative analysis of PET studies in oncology is affected by biological and technical factors, i.e., tracer kinetics, composition of tumor tissue, data acquisition and data analysis. Depending on the time-after-tracer injection, the PET signal represents initially intravascular [^{18}F]FDG activity followed by extracellular FDG equilibration during the first minutes. At later time points, the majority of the ^{18}F signal reflects intracellular FDG-6-phosphate (*30*). However, the lumped constant (LC), which allows calculation of glucose metabolism based on FDG uptake, has not been well investigated in tumor tissues. This parameter relates the steady-state phosphorylation rate of FDG to that of glucose and was determined first for brain tissue by means of the [^{14}C]2-deoxyglucose method (*31*). It was found to be different in other tissues such as the myocardium, but the LC was also not uniform among different brain regions, i.e., the hippocampus and cerebellum. Furthermore, the LC is increased in ischemic and postischemic tissue, and also dependent on blood glucose and insulin concentration (*32,33*). Therefore, it cannot be expected that tumors or metastases even in the same patients have the same lumped constant. Hence, FDG data may not be extrapolated to quantitative aspects of tumor glucose metabolism.

Another source of inaccuracy is the distribution of FDG in different body compartments. Fat, for example, has a lower FDG uptake than other tissues. Therefore, FDG uptake in tumors will be overestimated in heavy patients. Zasadny and Wahl have proposed the use of the lean body mass and Kim et al. suggested the use of the body surface area for correction of this effect (*14,15*). However, applying this correction method to our study population was not superior to other SUVs in order to differentiate benign from malignant breast tissue. These methods may be more helpful in patients who are significantly under- or overweight.

For comparison of tracer uptake in tumors of different patients, it is important to image during the plateau phase of tracer retention. Hamberg and colleagues showed that FDG uptake values varied widely with time in lung cancer patients (*16*). In this study, SUVs from breast tumors were obtained at 40–60 min after tracer injection. Assessment of dynamic data showed that the plateau phase was reached in 18 of 23 malignant breast tumors. However, some tumors showed increasing FDG accumulation up to 60 min after tracer injection. Since these tumors displayed high SUVs at this time window, no effect on the diagnostic accuracy to differentiate benign from malignant lesions has been observed. On the other hand, when comparing tracer uptake in the same patient, e.g., in therapy monitoring studies, increasing FDG accumulation over time requires careful timing of static PET imaging after tracer injection.

Effect of Blood Glucose Level

Due to the competition between the transport of endogenous glucose and FDG molecules into the cell, FDG uptake in cancer is sensitive to variation in blood glucose levels. Langen et al. investigated 15 patients with lung cancer and reported markedly decreased FDG uptake (41.8% ± 15%) when after glucose infusion plasma glucose levels were about double compared with those of fasting conditions (*23*). Wahl et al. also found that FDG uptake in breast cancer in rats was significantly reduced by continuous glucose infusion (*34*). However, the relationship between blood glucose level and FDG uptake in tumors is not yet fully known. For normalization of SUVs to blood glucose concentrations we assumed a linear relationship. Despite the fact that all patients fasted for at least 4 hr, blood glucose levels ranged from 44–126 mg/dl. However, none of these patients had diabetes and most had blood glucose levels close to the mean value. This may be one reason for the relatively small changes in diagnostic accuracy after applying blood glucose normalization.

Analysis of Dynamic PET Studies

Patlak and Blasberg introduced a theoretical model of blood-brain exchange for the analysis of multiple-time tissue uptake data (*10*). This approach is general and also valid in tumors if an unidirectional tracer transfer process predominates during the PET data acquisition period. Dynamic data acquisition for the assessment of time activity curves over the tumor and measurement of the tracer input function is necessary to calculate the tracer influx constant (K). Results of this study showed that using the FDG influx constant (K) did not improve the differentiation between benign and malignant breast tumors as compared with calculating SUV values. High s.d. in the Patlak analysis of benign tumors (Table 1) is most likely due to the small number of lesions (n = 12) and the flat slope of tracer uptake in benign tumors. On the other hand, the potential advantage of the Patlak analysis is that the determination of the influx constant does not require PET scanning at time of the plateau phase of tracer accumulation in tumors. Furthermore, if the input function is obtained from arterial blood pool in PET images, the Patlak analysis is not affected by scanner cross-calibration.

Effect of Tissue Heterogeneity

Relative contribution of malignant tumors range from a few transformed cells up to more than 90% of malignant cells. Due to the limited spatial resolution of PET imaging, the ^{18}F signal in tumors represents an average of FDG uptake in all tumor components. Kubota et al. showed higher FDG uptake in inflammatory cells than in malignant tumor cells using autoradiographic studies of tumors (*35*). On the other hand, nonmetabolic active components, i.e., necrotic tissue, fibrotic scar or mucine may reduce FDG uptake in tumors. To address this issue, several investigations have introduced methods that take into account FDG uptake in different components (*36*). However, metabolic analysis of radiotracer activity requires proper mathematical models. Thus far, there is no analysis method available to exactly describe FDG biokinetics in tumors.

Data Acquisition and Data Analysis

Concerning data acquisition and data analysis, attenuation of the emitted annihilation gamma rays, partial volume effect, patient movement during the PET scanning procedure as well as the placement of ROIs are the most relevant sources of inaccuracy in the evaluation of regional tracer uptake. Attenuation correction is necessary to obtain quantitative data in PET images. Furthermore, lack of attenuation correction leads to overestimation of tracer accumulation at the body surface and distortion in shape (*37*).

Partial volume effects caused by limited sampling and resolution results in underestimation of regional tracer uptake, predominantly in tumors smaller than twice the resolution of the imaging system (*38*). For appropriate correction, the necessary recovery coefficients are determined from phantom studies. In this study, spherical geometry of breast carcinomas was assumed because most of them showed circular, focally increased tracer uptake. However, this approach introduces biased results in nonspherical tumors. Furthermore, the assumption of homogeneous tumor tissue in such a correction may result in an undercorrection of partial volume effects. Information on tumor size is also necessary to perform partial volume correction.

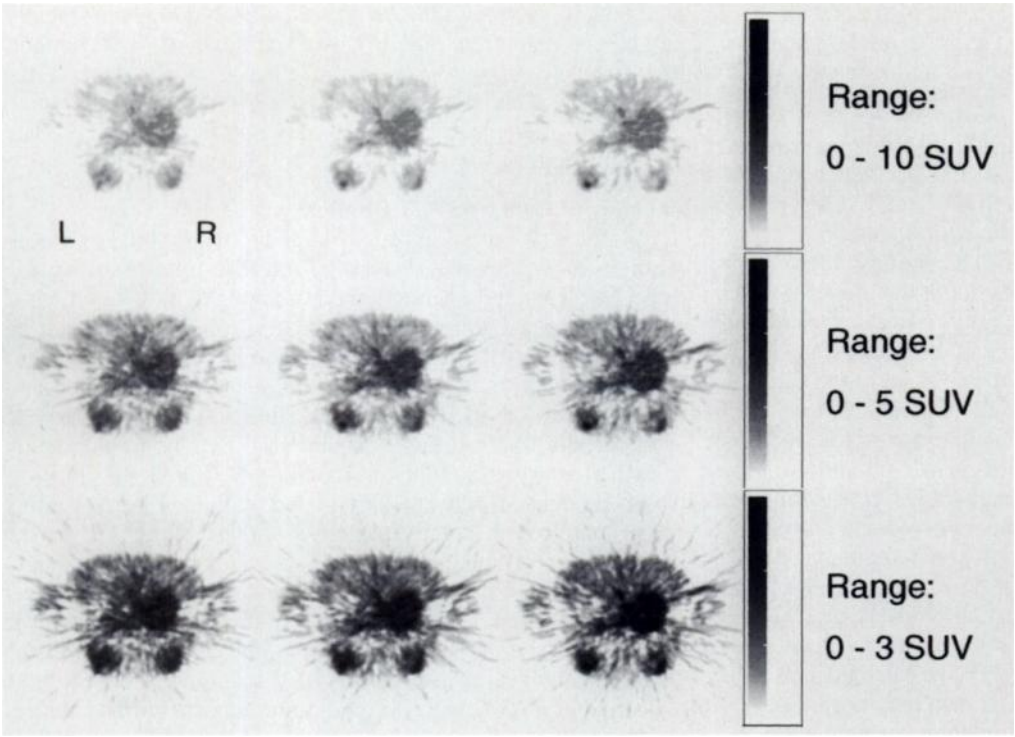

FIGURE 3. PET images demonstrating focally increased FDG uptake in the left breast, histologically proven as an invasive breast carcinoma. The display is normalized to SUVs using a linear gray scale of different ranges, simulating variability of visual image interpretation without quantitative data.

Using an automated approach, the tumor size was obtained by analysis of the axial plane activity profile of the lesion resulting in a close correlation to the size from histology (*26,27*). However, using this software, object size can be determined only in axial dimension, leading to false results in nonspherical tumors, as discussed above. On the other hand, automatic assessment of tumor size for subsequent partial volume correction may circumvent the need to obtain tumor size from other imaging modalities. Nevertheless, the major problem in breast imaging with PET is the detection of small tumors. Breast carcinomas smaller than 1 cm in diameter often cannot be visualized, and it is important to note that tumors without focally increased tracer uptake do not allow correction for partial volume effect using the imaging based correction factors.

Motion artifacts during the PET scanning procedure are another cause of error. In supine position, the chest wall movement is dependent on the patients respiration. Therefore, we studied the patients in prone position on a comfortable foam rubber support. A hole in the foam ensured that breasts could hang freely. This procedure reduced motion of the breast and optimized the evaluation of regional tracer uptake.

CONCLUSION

This study showed that various quantitative analysis methods provided stable parameters for differentiation of benign and malignant breast tumors. Visual image interpretation can be improved using quantitative standardization of data. Figure 3 in our manuscript simulated variable ways to display PET images of the breast for visual analysis by using different SUV ranges. One may clearly identify the carcinoma in the left breast using the gray scale ranging from 0–5 SUV (middle row). Using a display from 0–10 SUV, one may classify this tumor only as probable malignant, and using a display raging from 0–3 SUV one may report a suspicious breast mass at the contralateral breast. This example demonstrates the advantage of using quantitative data to compare regional FDG uptake in different patients with variable background activities. Quantitative data can be easily obtained and, therefore, quantitative assessment is recommended to complement image interpretation with the potential benefit of reduced interobserver variability.

ACKNOWLEDGMENTS

We gratefully acknowledge the effort of the cyclotron and radiochemistry staff. We also appreciate the excellent technical support of the PET technologists and the editorial help of Jodi Neverve and Ngoc Nguyen in the preparation of this manuscript.

REFERENCES

1. Kubota K, Matsuzwana T, Amemiya A, et al. Imaging of breast cancer with F-18 fluorodeoxyglucose and positron emission tomography. *J Comput Assist Tomogr* 1989;13:1097–1098.
2. Minn H, Soini I. (18-F) Fluorodeoxyglucose scintigraphy in diagnosis and follow up of treatment in advanced breast cancer. *Eur J Nucl Med* 1989;15:61–66.
3. Wahl RL, Cody RL, Hutchins GD, et al. Primary and metastatic breast carcinoma: initial clinical evaluation with PET with the radiolabeled glucose analogue 2-[F-18]-fluoro-2-deoxy-D-glucose. *Radiology* 1991;179:765–770.
4. Tse YN, Hoh CK, Hawkins RA, et al. The application of positron emission tomographic imaging with fluorodeoxyglucose to the evaluation of breast disease. *Ann Surg* 1992;11:359–377.
5. Nieweg ON, Kim EE, Wong W-H, et al. Positron emission tomography with fluorine-18-deoxyglucose in the detection and staging of breast cancer. *Cancer* 1993;71:3920–3925.
6. Hoh CK, Hawkins RA, Glaspy JA, et al. Cancer detection with whole-body PET using 2-[18-F]fluoro-2-deoxy-D-glucose. *J Comput Assist Tomogr* 1993;17:582–589.
7. Adler LP, Crowe JP, Al-Kaisi NK, et al. Evaluation of breast masses and axillary lymph nodes with (F-18) 2-deoxy-2-fluoro-D-glucose PET. *Radiology* 1993;187:743–750.
8. Avril N, Dose J, Jänicke F, et al. Metabolic characterization of breast tumors with positron emission tomography using F-18 fluorodeoxyglucose. *J Clin Oncol* 1996;14: 1848–1857.
9. Kopans DB, Meyer JE, Sadowsky N. Breast Imaging. *N Engl J Med* 1984;310:960–967.
10. Patlak CS, Blasberg RG, Fernstermacher JD. Graphical evaluation of blood-to-brain transfer constants from multiple-time uptake data. *J Cereb Blood Metab* 1983;3:1–7.
11. DiChiro G, Brooks RA. PET quantitation: blessing and curse. *J Nucl Med* 1988;29: 1603–1604.
12. Strauss LG, Conti PS. The applications of PET in clinical oncology. *J Nucl Med* 1991;32:623–648.
13. Hawkins RA, Choi Y, Huang S-C, et al. Quantitating tumor glucose metabolism with FDG and PET. *J Nucl Med* 1992;33:339–344.
14. Zasadny KR, Wahl RL. Standardized uptake values of normal tissues at PET with 2-[fluorine-18]-fluoro-2-deoxy-D-glucose: variations with body weight and a method for correction. *Radiology* 1993;189:847–850.
15. Kim CK, Gupta NC, Chandramouli B, et al. Standardized uptake values of FDG: body surface area correction is preferable to body weight correction. *J Nucl Med* 1994;35: 164–167.
16. Hamberg LM, Hunter GJ, Alpert NM, et al. The dose uptake ratio as an index of

glucose metabolism: useful parameter or oversimplification? *J Nucl Med* 1994;35:1308–1312.
17. Lowe VJ, Hoffmann JM, DeLong DM, et al. Semiquantitative and visual analysis of FDG-PET images in pulmonary abnormalities. *J Nucl Med* 1994;35:1771–1776.
18. Keyes JWJ. SUV: standard uptake or silly useless value? *J Nucl Med* 1995;36:1836–1839.
19. Minn H, Joesuu H, Ahonen A, et al. Fluorodeoxyglucose imaging: a method to assess the proliferative activity of human cancer in vivo; comparison with DNA flow cytometry in head and neck tumors. *Cancer* 1988;61:1776–1781.
20. Strauss LG, Clorius JH, Schlag P, et al. Recurrence of colorectal tumors: PET evaluation. *Radiology* 1989;170:329–332.
21. Knopp MV, Strauss LG, Haberkorn U, et al. Optimizing therapy management in unresectable bronchiogenic carcinoma by metabolic imaging with PET. *J Nucl Med* 1990;31:766.
22. Haberkorn U, Strauss LG, Dimitrakopoulou A, et al. PET studies of fluorodeoxyglucose metabolism in patients with recurrent colorectal tumors receiving radiotherapy. *J Nucl Med* 1991;32:1485–1490.
23. Langen K-J, Braun U, Kops ER, et al. The influence of plasma glucose levels on fluorine-18-fluorodeoxyglucose uptake in bronchial carcinomas. *J Nucl Med* 1993;34:355–359.
24. Laubenbacher C, Saumweber D, Wagner-Manslau C, et al. Comparison of fluorine-18-fluorodeoxyglucose PET, MRI and endoscopy for staging of head and neck squamous-cell carcinomas. *J Nucl Med* 1995;36:1747–1757.
25. Hamacher K, Coenen HH, Stöcklin G. Efficient stereospecific synthesis of nocarrier-added 2-(F-18)-fluoro-2-deoxy-D-glucose using aminopolyether supported nucleophilic substitution. *J Nucl Med* 1986;27:235–238.
26. Weber W, Schad D, Römer W, et al. Fluorine-18 FDG-PET in solitary pulmonary nodules: determination of tumor size and correction of partial volume effect. *J Nucl Med* 1995;36:95P.
27. Schad D, Ziegler S, Weber W, et al. Quantitative Ermittlung der Aktivitätskonzentration von tumor-PET-Datensätzen mittels automatischer Grö§enBestimmung und Partialvolumenkorrektur [Abstract]. *Nuklearmedizin* 1996;35:A89.
28. Hanley JA, McNeil BJ. The meaning and use of the area under a receiver operating characteristic (ROC) curve. *Radiology* 1982;143:29–36.
29. Metz CE. Basic principles of ROC analysis. *Semin Nucl Med* 1978;8:283–298.
30. Gallagher BM, Fowler JS, Gutterson NI, et al. Metabolic trapping as a principle of radiopharmaceutical design: some factors responsible for the biodistribution of (^{18}F) 2-deoxy-2-fluoro-D-glucose. *J Nucl Med* 1978;19:1154–1161.
31. Sokoloff L, Reivich M, Kennedy C, et al. The [C-14] deoxyglucose method for the measurement of local cerebral glucose utilization: theory, procedure and normal values in the conscious and anesthetized albino rat. *J Neurochem* 1977;28:897–916.
32. Buxton DB, Schelbert HR. Measurement of regional glucose metabolic rates in reperfused myocardium. *Am J Physiol* 1991;261:2058–2068.
33. Ng CK, Holden JE, DeGrado TR, et al. Sensitivity of myocardial fluorodeoxyglucose lumped constant to glucose and insulin. *Am J Physiol* 1991;260:593–603.
34. Wahl RL, Henry CA, Ethier SP. Serum glucose: effects on tumor and normal tissue accumulation of 2-[F-18]-fluoro-2-deoxy-D-glucose FDG in rodents with mammary carcinoma. *Radiology* 1992;183:643–647.
35. Kubota R, Yamada S, Kubota K, et al. Intratumoral distribution of fluorine-18-fluorodeoxyglucose in vivo: high accumulation in macrophages and granulation tissue studied by microautoradiography. *J Nucl Med* 1992;33:1972–1980.
36. Blomqvist G, Lammertsma AA, Mazoyer B, et al. Effect of tissue heterogeneity on quantification in positron emission tomography. *Eur J Nucl Med* 1995;22:652–663.
37. Zasadny KR, Kison PV, Quint LE, et al. Quantification of systematic distorsion in nonattenuation corrected FDG-PET images in patients with untreated lung cancer. *J Nucl Med* 1995;36:5P.
38. Hoffmann EJ, Huang S, Phelps ME. Quantitation in positron emission computed tomography: effect of object size. *J Comput Assist Tomogr* 1979;3:299–308.

Clinical Significance of Hepatic Visualization on Iodine-131 Whole-Body Scan in Patients with Thyroid Carcinoma

June-Key Chung, Yong Jin Lee, Jae Min Jeong, Dong Soo Lee, Myung Chul Lee, Bo Yeon Cho and Chang-Soon Koh
Departments of Nuclear Medicine and Internal Medicine, Seoul National University Hospital, Seoul, Korea

The purpose of this study was to evaluate the frequency and clinical significance of diffuse hepatic uptake on ^{131}I whole-body scan in 399 patients (53 males, 346 females) with well-differentiated adenocarcinomas of the thyroid. **Methods:** Two hundred and ninety-one diagnostic scans were performed 2 days after the administration of 74–370 MBq (2–10 mCi) ^{131}I, and 824 post-therapy scans were done 3–5 days after the administration of 1.11–7.4 GBq (30–200 mCi) ^{131}I. There was no evidence of liver metastasis in these patients. Liver and thyroid visualization on each ^{131}I scan were graded from 0–4. To evaluate the incorporation of radioiodine to thyroglobulin and thyroid hormones, a patient's serum was extracted by 80% ethanol/20% trichloroacetic acid solution and analyzed by silica gel thin-layer chromatography. **Results:** Diffuse hepatic uptake (>Grade 2) was definitely seen in 239 of 399 (59.9%) of the patients and 397 of 1115 (35.6%) of the studies. In the diagnostic scans, 36 (12.0%) showed uptake in the liver. In post-therapy scans, however, the incidence of liver uptake increased according to increased doses of ^{131}I (39.1% with 1.11 GBq, 61.5% with 2.775–3.7 GBq and 71.3% with 5.55–7.4 GBq). The more that uptake appeared in the residual thyroid, the more it appeared in the liver. There were 13 patients whose scans showed metastatic and liver uptake without any thyroid uptake. Fifteen patients showed diffuse liver uptake without uptake by the thyroid or metastasis. Follow-up studies of seven of these patients revealed metastatic lesions. Liver uptake on scan related to the fraction of ^{131}I-labeled thyroglobulin in the serum. **Conclusion:** Diffuse liver uptake indicated functioning thyroid remnant or metastasis. In a few cases, liver uptake without uptake by the thyroid or metastasis on whole-body scans suggests hidden metastases.

Received Aug. 28, 1996; revision accepted Jan. 7, 1997.
For correspondence or reprints contact: June-Key Chung, MD, Department of Nuclear Medicine, Seoul National University Hospital, 28 Yungun-dong, Chongno-gu, Seoul 110-744, Korea.

Key Words: liver; iodine-131 whole-body scan; thyroid cancer; metastasis

J Nucl Med 1997; 38:1191–1195

Whole-body ^{131}I scan has been used to evaluate patients with well-differentiated thyroid adenocarcinomas after operation and ablation therapy. Normally, radioactive iodine accumulates in organs, including residual thyroid tissue, the stomach, intestine, salivary gland and urinary bladder that secrete and concentrate iodide (*1*). Several studies have been published reporting diffuse liver uptake of ^{131}I in thyroid carcinomas after surgery, detected either during diagnostic procedures or after the administration of ablative doses of ^{131}I (*2–6*). Pochin suggested that diffuse liver uptake was mainly due to the metabolism of

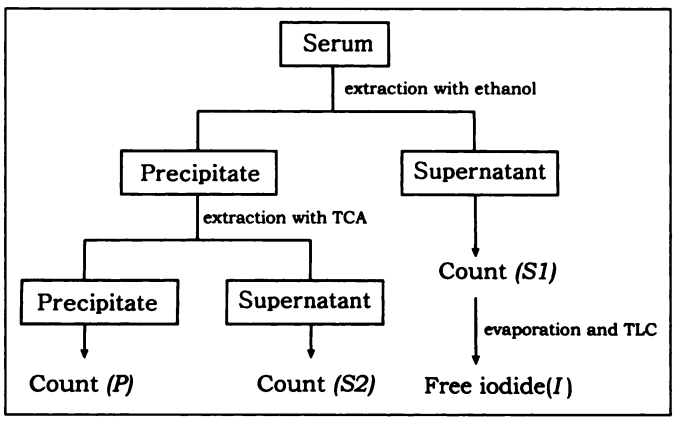

FIGURE 1. Scheme and interpretation of patient's serum analysis.